Self-Consistent, Integrated, Advanced Tokamak Operation on DIII–D

M.R. Wade,[1] M. Murakami,[1] T.C. Luce,[2] J.R. Ferron,[2] C.C. Petty,[2] D.P. Brennen,[3] A.M. Garofalo,[4] C.M. Greenfield,[2] A.W. Hyatt,[2] R. Jayakumar,[5] R.J. La Haye,[2] L.L. Lao,[2] J. Lohr,[2] P.A. Politzer,[2] R. Prater,[2] and E.J. Strait[2]

[1]Oak Ridge National Laboratory, Oak Ridge, Tennessee, 37831 USA
 email: wade@fusion.gat.com
[2]General Atomics, P.O. Box 85608, San Diego, California, 92186-5608 USA
[3]Oak Ridge Institute for Science Education, Oak Ridge, Tennessee 37831 USA
[4]Columbia University, New York
[5]Lawrence Livermore National Laboratory, Livermore, California 94551 USA

Abstract. Recent experiments on DIII-D have demonstrated the ability to sustain plasma conditions that integrate and sustain the key ingredients of Advanced Tokamak (AT) operation: high β with $q_{min} \gg 1$, good energy confinement, and high current drive efficiency. Utilizing off-axis ($\rho = 0.4$) electron cyclotron current drive (ECCD) to modify the current density profile in a plasma operating near the no-wall ideal stability limit with $q_{min} > 2.0$, plasmas with $\beta \approx 2.9\%$ and 90% of the plasma current driven non-inductively have been sustained for nearly 2 s (limited only by the duration of the ECCD pulse. Separate experiments have demonstrated the ability to sustain a steady current density profile using ECCD for periods as long as 1 s with β = 3.3 % and > 90% of the current driven non-inductively.

I. Introduction

The economical generation of electricity via fusion energy is predicated on maximizing the energy output per unit cost, averaged over the lifetime of the device. The attractiveness of any fusion power system therefore relies on providing high power density with low recirculating power while operating with a high duty factor. Within the worldwide magnetic fusion energy effort, two approaches are presently being pursued, the primary distinguishing feature being how the plasma current I_p is generated and maintained. The first approach generates the majority of the plasma current from Ohmic drive, resulting in an inherently pulsed device (the so-called conventional tokamak approach). The second approach strives to generate the entirety of the plasma current from non-inductive sources and therefore extrapolates to devices that are in principle capable of steady-state operation (the so-called Advanced Tokamak approach). While the conventional tokamak approach has been validated by experiments worldwide [1], the feasibility of achieving and sustaining Advanced Tokamak (AT) conditions is yet to be proven. A major objective of the DIII–D AT research program is demonstrating that plasma conditions can be achieved and sustained in which the plasma current is generated solely via the self-generated "bootstrap current" [2] ($I_{BS} = f_{BS} I_p$) and other non-inductive sources while maintaining acceptable fusion power density and fusion gain. A further goal is to establish the physics basis of the obtained regimes such that extrapolation to future devices can be more confidently made.

Over the past several years, the Advanced Tokamak (AT) program on DIII–D has made significant progress towards demonstrating integrated plasma operation that simultaneously achieves high non-inductive current fractions and high fusion power density. This program's primary goal is to develop plasma scenarios that self consistently integrate and sustain the key ingredients of Advanced Tokamak (AT) operation: high β at high q_{min}, good plasma confinement, and high current drive efficiency. In recent years, significant progress has been made in understanding the interplay among these elements from an experimental, theoretical, and modeling perspective. Using this knowledge, recent experiments have demonstrated the ability the combine these elements simultaneously. Utilizing off-axis ($\rho = 0.4$) ECCD to modify the current density profile in a plasma operating near the no-wall ideal stability limit with $q_{min} > 2.0$, plasmas with $\beta \approx 2.9\%$ and 90% of the plasma current driven non-inductively have been produced and sustained for nearly 2 s (limited only by the duration of the ECCD pulse). While many experiments worldwide (including many done on DIII–D) have demonstrated the key components individually, this is the first experiment to self consistently integrate these elements simultaneously. In these discharges, ECCD is integral in

producing negative central magnetic shear, helping to form a weak internal transport barrier (for both ions and electrons) that is maintained in the presence of a fully developed H–mode edge with Type I ELMs. Separate experiments using ECCD have also shown the ability to sustain a nearly constant current density profile for ~ 1 s with $q_{min} > 1.5$. In this case, $\beta \approx$ 3.3% is maintained with ~ 95% of the plasma current driven non-inductively.

These two cases, as well as supporting information related to the extension of these results to fully non-inductive current drive, are discussed in this paper. First, recent results demonstrating the ability to modify and control the current density profile using ECCD are discussed in Section II. In Section III, issues related to maximizing the total non-inductive current are discussed along with a discussion of the future prospects for fully non-inductive AT operation in DIII–D.

II. Controlling the Current Profile

The primary distinguishing feature of advanced tokamak plasmas relative to conventional tokamak plasmas is the current density profile. In conventional tokamak operation, the current density is allowed to resistively relax such that $<E_{||}>$ is constant across the plasma column. Since the primary constituent of the current profile is the Ohmic current $J_{ohm} = \sigma E_{||}$ (where σ is the plasma conductivity and $E_{||}$ is the parallel electric field), the current density is strongly peaked on-axis, resulting in a monotonic q profile with $q_0 \lesssim 1$. In such a case, turbulent growth rates are sufficiently large that stabilization processes such as E×B shear are not large enough to cause significant suppression of the turbulence, resulting in moderate levels of transport. Furthermore, $q_0 < 1$ leads to increased probability of sawteeth or fishbones, which are known to produce seed islands for neoclassical tearing modes (NTMs), thereby severely limiting the sustainable β. Actively controlling the current profile offers many advantages. From a confinement and transport standpoint, theoretical studies indicate that it is favorable to maintain either low or high magnetic shear over a substantial portion of the plasma radius so as to maximize stability to MHD-driven and ion temperature gradient (ITG) driven modes [3–6]. It is also favorable, though not required if high β_N can be achieved, to operate at high q_{min} in order to maximize the self-generated bootstrap current. Therefore, one of the major steps towards achieving sustained AT operation is demonstrating the ability to control the current profile in a high β plasma.

The ability to do this has been demonstrated in two separate experimental cases on DIII–D. In the first case (described in Section II.A), off-axis ECCD has been used to modify the current density profile in a high β plasma with $q_{min} > 2$. In the second case (described in Section II.B), off-axis EECD has been used to sustain a nearly stationary current density profile for up to 1 s. These experimental results validate simulation results (carried out prior to the experiment) which predicted the ability to modify the current profile using off-axis ECCD. This provides confidence that ECCD can be used effectively and predictably for current profile control both in the DIII–D AT program and in future devices.

A. Modification of the current profile at high β with $q_{min} > 2$

The temporal evolution of a discharge in which off-axis ECCD has been used to modify the current profile in a high β plasma is shown in Fig. 1. In this case, an L-H transition is induced early in the current ramp in order to slow down the penetration of the current density such that $q_{min} > 2$ at the end of the current ramp. Just after the end of the current ramp, feedback control of the neutral beam injection (NBI) system is initiated and commanded to regulate the diamagnetic flux to a level that corresponds to $\beta_N \sim 2.8$ for the remainder of the discharge. Once high β is established, approximately 2.5 MW of EC power from five 110 GHz gyrotrons is applied at 1.5 s. To achieve off-axis current drive, the EC waves are steered toroidally to generate current parallel to the plasma current and poloidally to damp in a narrow region around the normalized radius $\rho = 0.4$ on the inboard side of the magnetic axis. A significant increase in negative magnetic shear is produced within 500 ms of the

initiation of ECCD and then maintained for the duration of the ECCD pulse (2 s). Comparisons with cases using radially launched ECH (therefore no current drive) at the same deposition location indicate that the current profile modification is almost entirely due to ECCD as the ECH case shows little difference from an NBI-only case.

Equilibrium reconstructions also show peaking of current density profile near $\rho = 0.4$ starting approximately 400 ms after the initiation of ECCD. Coincident with these changes, the current density in the core plasma is reduced, resulting in a strongly reversed q profile with $q_{min} = 2.0$ and $q_0 = 5.0$ at 2.7 s. Analysis of the MSE response to the ECCD indicates an ECCD driven current of 130 ± 40 kA. This agrees well with the CQL3D Fokker-Planck code [7] prediction of 120 kA. The obtained current drive corresponds to a normalized CD efficiency

Fig. 1. Plasma parameters versus time for a discharge (111203) in which ECCD is used to modify the current profile:(a) Plasma current (MA), neutral beam injected power (10 MW), line-averaged density (10^{20} m^{-3}), (b) β_N (darker trace), $4 \times \ell_i$ (lighter trace), (c) q_0 (upper trace), q_{min} (lower trace), (d) central ion and electron temperature and (e) divertor D_α(a.u.).

$\zeta = 33\ n_{20}I_AR_m/(P_WT_{keV}) = 0.26$ (10^{20} A/Wm^{2}keV), which is consistent with previous estimates of what is required for successful implementation of the AT research program on DIII–D in future years. The ECCD efficiency in this case is favorably affected by a reduction in trapped electron effects resulting from: (a) EC absorption on the inboard side, and (b) high electron beta which moves the resonance location away from the trapping boundary in velocity space [8]. The efficiency is also favorably affected by excellent density and impurity control. The line-averaged density in this case is maintained at $n_e = 3.4 \times 10^{19}$ m^{-3} while Z_{eff} in the core in maintained below 2.0. No evidence of impurity accumulation in the plasma center is observed.

The measured Ohmic current $J_{Ohm} = \sigma\ E_{||}$, which is determined from the temporal evolution of the poloidal magnetic flux ($<E_{||}> \sim d\psi/dt$) and assuming neoclassical resistivity $\sigma = \sigma_{neo}$ [9], amounts to approximately 10% of the total current. This agrees well with the calculated non-inductive sources, which indicate that 10% of the current is supplied by ECCD, 55% from the bootstrap current, and 25% from NBCD. It is anticipated that broadening of the ECCD deposition location through steering of the separate EC mirrors should reduce this Ohmic current peak somewhat while improving the current drive alignment in the plasma center.

The total bootstrap current is approximately 20% higher in the ECCD case relative to the reference cases as a result of modifications to the plasma profiles attributable to the effect of ECCD. These changes in the profiles are observed to occur coincidentally with the changes in the magnetic shear in the core. Increases in both the electron and ion temperature as well as electron density and toroidal rotation velocity are observed (Fig. 2), indicating an improvement in confinement in all transport channels. These increases occur primarily within the magnetic shear reversal region $0.1 < \rho < 0.5$. The improved confinement is confirmed by transport analysis, which indicates significant decreases in the ion thermal diffusivity χ_i and momentum diffusivity χ_ϕ while more modest decreases are inferred for the electron thermal diffusivity χ_e and particle diffusivity D_e (Fig. 3). Since the primary difference between the ECCD case and the other cases is the evolution of the current density profile, it is believed that these improved transport properties result primarily from the increase in negative magnetic shear induced by the ECCD. Preliminary analysis using the GKS gyro-kinetic code [10] indicates that both negative magnetic shear and E×B shear are stabilizing in this case. The former is particularly important for electron transport since magnetic shear stabilization reduces turbulence growth rates over a wide range of turbulence scale lengths, in
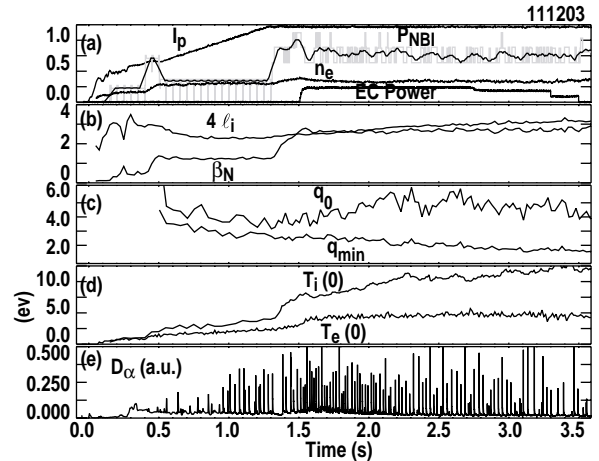
contrast to E×B shear, which primarily affects long-wavelength turbulence. This improvement in transport is reflected in the overall energy confinement with H_{89} = 2.2 and H_{98y2} = 1.3. Here, H_{98y2} is the energy confinement enhanced factor relative to the multi-machine H–mode scaling relation $H_{98y2} = \tau_E/\tau_{E,ITER98y2}$.

The simultaneous attainment of high β, good ECCD efficiency, and good confinement is noteworthy in this case, as it represents first successful integration of these key elements. In addition, the kinetic and current density profiles obtained at 2.7 s exhibit many of the features elucidated by theoretical and modeling studies that have focussed on AT regimes, in particular, strong negative central shear and an internal transport barrier.

B. Sustaining the current profile at high β with $q_{min} > 1.5$

Separate experiments have demonstrated the ability to sustain a nearly stationary current density profile for up to 1 s in plasmas with $q_{min} > 1.5$. Operationally, the primary difference between the high q_{min} case discussed in Section II.A and the discharge discussed in this section (which has q_{min} below 2) is the timing of the high power and ECCD phases. In this case, the high power phase is delayed to allow the current density to penetrate more fully to the plasma center, thereby producing a lower q_{min} target. In the case shown in Fig. 4, high power injection begins at 2.8 s with q_{min} =

Fig. 2. Comparison of the measured profiles in the ECCD case (darker traces) and ECH case (lighter cases) at 2.7 s: (a) q profile; (b) electron density; (c) ion (top) and electron (bottom) temperature; and (d) toroidal rotation.

Fig. 3. Comparison of the inferred diffusivities using TRANSP in the ECCD case (darker traces) and the ECH (lighter traces): (a) electron thermal diffusivity χ_e, (b) ion thermal diffusivity χ_i, (c) particle diffusivity D_e, and (d) momentum diffusivity χ_ϕ.

1.7. Subsequently, β_N = 3.1 is maintained by feedback control of the NBI power (average of 9.5 MW). As in the higher q_{min} case, approximately 2.5 MW of co-directed ECCD resonant on the inboard midplane at ρ = 0.4 is applied starting at 3.0 s. Between 3.0 and 4.0 s, the current density profile is observed to be nearly constant with q_0 ~ 2.1 and q_{min} ~ 1.7, suggesting that the current density profile is nearly stationary during this period. Equilibrium reconstructions indicate both the current density profile and overall pressure profile as well as the density and temperature profiles are nearly stationary during this period. This nearly stationary phase is ended at 4.0 s by the destabilization of a small m=5/n=3 NTM. It appears that this NTM is destabilized as q_{min} reaches 1.67, indicating that a small amount of current diffusion is still occurring throughout this period. The current profile evolution between 3.0 and 4.0 s is consistent with the measured Ohmic current, which is shown in Fig. 5. The Ohmic current is significantly reduced during the ECCD phase (t = 3.7 s) relative to that measured just before the high power phase (t = 2.7 s). The Ohmic current in the ECCD phase is nearly zero in the inner half of the plasma, indicating that the current in this region of the plasma is supplied fully by the non-inductive sources. Some Ohmic current remains in the outer half of plasma, but this only amounts to ~ 5% of the total current. Hence, 90% of the plasma is driven non-inductively in this case with ~ 65% of the plasma current provided by bootstrap current, ~ 23% by neutral beam current drive, ~ 7% by ECCD. The edge loop voltage during this period is ~ 50 mV, further indicating that there is only a small amount of Ohmic drive. Since the remaining Ohmic current is peaked off-axis, we believe it will possible to replace this current with careful optimization of the ECCD deposition location in
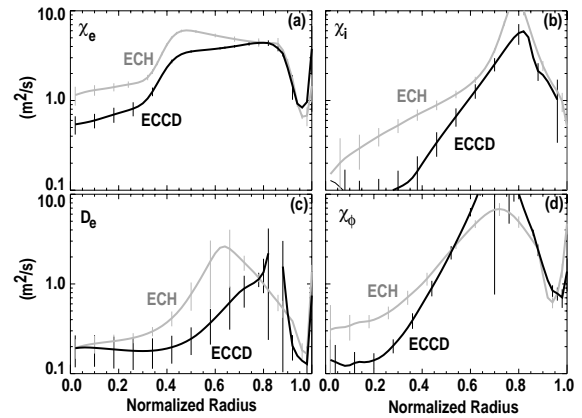
combination with higher β operation. The kinetic profiles in this case exhibit no signs of internal transport barrier formation, but transport analysis indicates that the local transport is reduced over the entire plasma radius relative to a standard, ELMing H–mode discharge. This is reflected in an energy confinement quality that is somewhat better than the typical ELMing H–mode with $H_{89} = 2.4$ and $H_{98y2} = 1.3$.

III. Maximizing The Total Non-Inductive Current

Obtaining fully non-inductive operation economically is predicated on obtaining a high bootstrap current fraction ($f_{BS} \propto q \, \beta_N$), which favors high β_N operation with elevated q values (typically, $q_{min} > 1.5$, $q_{95} > 4$). In order to maintain an adequate fusion power density ($\beta \propto \beta_N/q$) and fusion gain ($\beta \, \tau_E \propto \beta_N \, H_{89}/q^2$) at these higher q values, operation well above the generally accepted long pulse limits on both stability ($\beta_N = 3$) and confinement ($H_{89} = 2$) is required. Furthermore, to increase the fraction of current supplied from other non-inductive sources, good current drive efficiency is required, implying a need for high electron T_e and low density n_e, since the ability to produce current drive I_{CD} for a given amount of current drive power scales as $I_{CD} \propto T_e \, P_{CD}/n_e$.

Recent experiments have demonstrated the ability to achieve stable operation with β_N well above the no-wall, ideal, n=1 β limit [11]. Access to high β in these cases is predicated on simultaneously stabilizing resistive wall modes (RWMs) via rotational stabilization of the RWMs and avoiding NTMs through careful tailoring of the current profile. The best cases have been achieved with a current density profile similar to that sustained in Fig. 4 with q_0 slightly above 2 and q_{min} slightly below 2. In these cases, $\beta_N > 4$ (which is near the ideal-wall n=1 β limit) is maintained for several energy confinement times with the duration only limited by resistive relaxation of the current profile to an unstable state. These discharges have comparable performance to that achieved in previous studies [12,13] but was achieved in a plasma shape conducive to coupling to the upper divertor in DIII–D ($\kappa = 1.85$, $\delta = 0.65$, $q_{95} = 4.1$, DND) as opposed to the optimized shape used previously ($\kappa = 2.0$, $\delta = 0.9$, $q_{95} = 5.6$, DND). Because of the double null divertor shape, adequate particle control is not obtained, since the lower divertor of DIII–D is not optimized for pumping high elongation κ, high δ plasmas. Hence, while high β is obtained, a low current drive efficiency is obtained. This is depicted graphically in Fig. 6, in which β_p (a measure of the obtainable bootstrap current) is plotted versus the relative current drive efficiency parameter $\eta_{ECCD} \propto (T_e/n_e R)\beta_e^{1/2}$. The additional factor $\beta_e^{1/2}$ here is based on extensive studies of the various physics phenomenon governing ECCD current drive efficiency that have been conducted on DIII–D and which are summarized in Ref. [8]. These studies indicate that the normalized current drive efficiency increases as approximately $\beta_e^{1/2}$, arising from Doppler shifting of the resonance location in
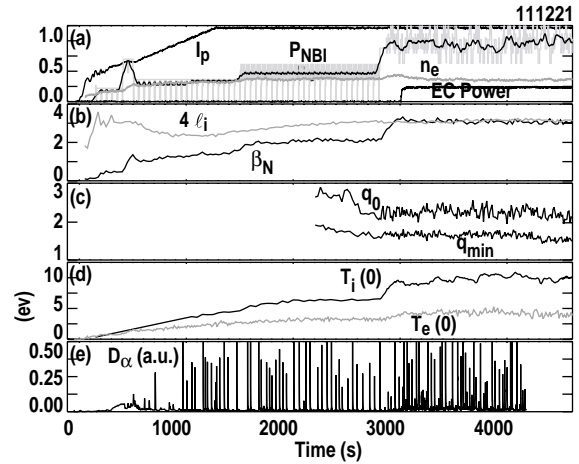
Fig. 4. Plasma parameters versus time for a discharge (111221) in which ECCD is used to sustain the current profile: (a) plasma current (MA), neutral beam injected power (10 MW), line-averaged density (10^{20} m^{-3}), (b) β_N (darker trace), $4\times\ell_i$ (lighter trace), (c) q_0 (upper trace), q_{min} (lower trace), (d) central ion and electron temperature and (e) divertor D_α(a.u.).
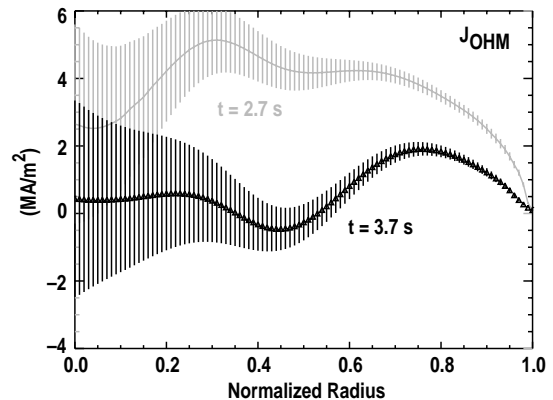
Fig. 5. Comparison of the measured Ohmic current density profile just before the high power phase (t = 2.7 s) and during the ECCD phase (t = 3.7s) for the discharge shown in Fig. 4.

velocity space so that the EC power is absorbed by electrons that are further away from the trapped electron boundary than would be the case with $\beta_e = 0$. The discharge described above (#106795) lies in the upper left hand corner of Fig. 6, having a β_p value consistent with the DIII–D AT target, but η_{ECCD} is considerably below the desired level due to the high electron density. Included in this figure also are the ECCD discharges shown in Fig. 1 (# 111203) and Fig. 4 (#111221). In the ECCD cases, η_{ECCD} is considerably higher (within a factor of two of the desired level) but $\beta_p < 1.5$ due to the reduced β in these cases. Increasing β while maintaining good density control should allow improvements in both β_p and η_{ECCD} in the ECCD cases.

Fig. 6. β_p versus (T_e/n_e) $\beta_e^{1/2}$ at $\rho = 0.5$. All discharges have $\beta_N > 4$ ℓ_i. Star denotes AT target design point, with $T_e \sim T_i$.

Studies have shown that sufficient exhaust efficiency can be obtained in slightly unbalanced upper single-null configuration with $\Delta R_{sep} > 5$ mm. Here, ΔR_{sep} is the radial distance at the midplane between field lines that connect to the two divertor nulls. By convention, positive values of ΔR_{sep} mean the upper-null is dominant while negative is lower-null dominant. Typically, an increase in ΔR_{sep} from 0 to 1 cm without making any other changes in the plasma shaping algorithm results in a 10% reduction in the achievable β as well as a reduction in q_{95}. The reduced β limit is consistent with systematic studies that show a decrease in the experimentally achievable β_N as q_{95} decreases. By increasing the triangularity and elongation in the lower divertor (by pulling the lower divertor X–point radially inward and vertically down), the q_{95} of the DN case can be recovered with $\Delta R_{sep} = 1$ cm. Using this slightly unbalanced upper single-null magnetic configuration, experiments have demonstrated the ability to simultaneously obtain good density control with β_N approximately the same as the best DN cases. However, the duration of the high performance phase is generally reduced due to an earlier onset of a m=2/n=1 NTM.

Another path to increasing the bootstrap current is by operating at higher q. To obtain adequate fusion power density and fusion gain, $q_{95} < 5$ is required, making it necessary to operate with $q_{min} \gg 1$ to obtain high bootstrap current. This approach relies on the assumption that the attainable β_N is not a strongly decreasing function of q_{min}. Because of the broader current profiles associated with higher q_{min} operation, it is expected that the no-wall β_N limit would decrease as q_{min} increases for a given pressure profile. However, stability calculations indicate that wall stabilization is more effective at high q_{min} as the location of the unstable modes moves radially outward, suggesting that a higher ideal, n = 1 limit is obtainable at higher q_{min}. To assess this, experiments have been conducted to separately measure the no-wall β_N limit and the maximum attainable β_N at different values of q_{min}. The no-wall β_N limit is determined by taking advantage of the strongly non-linear plasma response to an asymmetric magnetic field when operating near the no-wall β_N limit [14]. To take advantage of this non-linearity experimentally, discharges are established which have the ambient magnetic error minimized by external error field correction coils and β_N regulated to the desired value by feedback control of the neutral beam power. At a prescribed time, the external error field correction coils are disabled, which has the effect of turning on the ambient error field. On successive shots, β_N is then systematically scanned to determine the no-wall β_N limit, assuming that cases with large reductions in the plasma rotation are above the limit and those with minimal reductions are below the limit. The no-wall β_N limit determined in this manner for current profiles with varying values of q_{min} is shown in Fig. 7. In all of these cases, the magnetic shear in the plasma core is nearly the same with q_0–q_{min} = 0.5. It is evident from Fig. 7 that the no-wall β_N limit determined in this way decreases strongly with q_{min}. The maximum attainable β_N limit (obtained using full RWM
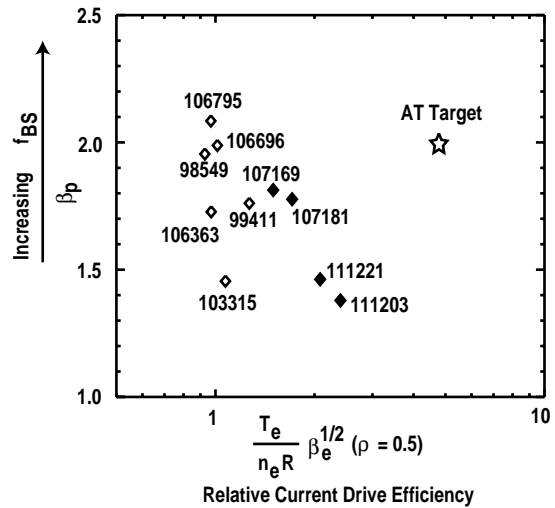
stabilization) at the extremes of the scan in q_{min} is also shown in Fig. 7. This decrease in β_N as qmin increases leads to a weak dependence of the bootstrap current fraction on q_{min}.

Note that no effort has been made in the high q_{min} case to determine if a higher β limit can be obtained by optimization of the pressure profile, which is known to be important to n=1 stability. While the β limit in the low q_{min} case is due to the destabilization of a NTM as q_{min} approaches 1.5, the cause of the low β limit is still under investigation.

V. Discussion

Having simultaneously combined the necessary elements for achieving steady-state, AT operation, the discharges discussed in Section II should offer excellent starting points for realization of a fully non-inductive AT demonstration in the near future in DIII–D. Both of these cases achieve β values near or above 3% and produce over 90% of the plasma current non-inductively. The primary challenge in extending these discharges to fully non-inductive operation appears at present to be obtaining stable operation at higher β. Higher β operation would afford both higher bootstrap fractions as well as higher current drive efficiency for the ECCD system (due to an increase in β_e). Ultimately, one would like to simultaneously optimize both the bootstrap current and the current drive efficiency, moving towards the target depicted in the upper right hand corner of Fig. 6. Increasing β while maintaining good density control should allow improvements in both β_p and η_{ECCD}.

Fig. 7. Dependence of the measured no-wall β_N limit (through method described in text) and maximum attainable β_N on q_{min}. ECCD cases from Figs. 1 and 4 are also shown.

This poses a significant challenge in the high q_{min} case discussed in Section II.A since the attainable β in discharges with similar current profiles appears to be limited (Fig. 7). The β limit in this case appears to be due to rapidly growing tearing modes rather than resistive wall modes, lending some hope that through proper tailoring of the current profile such modes can be avoided. However, a recent work has shown the destabilization of NTMs in these AT discharges is consistent with a theory that predicts the destabilization of the NTM by a rapid increase in Δ' as an ideal stability boundary is approached [15]. If this theory is correct, the occurrence of such NTMs may simply be symptomatic that the ideal n=1 β limit is being approached and that a further increase in β is not possible. Further studies are necessary to clarify this issue and determine whether higher β values can be obtained reliably. Of particular importance in such a study will be developing an understanding of the linkage between the current density profile and the transport profile. A further consideration is the limitations imposed by non-ideal MHD instabilities such as resistive interchange modes, which in certain circumstances, can limit β well below the ideal β limit. These are important details that may limit the extent to which strongly inverted q profiles with high q_{min} can be used to obtain 100% bootstrap current driven plasmas.

The most expeditious path to fully non-inductive operation appears to be discharges with current profiles similar to those obtained in the cases discussed in Section II.B. With this current profile (q_{min} slightly above 2, q_0 slightly below 2), operation well above the no-wall ideal β limit as well as the ability to maintain a stationary current profile have been demonstrated. The successful integration of these elements should result in high β, fully non-inductive plasma operation. This has been validated by recent simulation studies. These simulations take as input the experimentally measured transport profiles and then self-consistently solve the kinetic and current transport equations, evolving the transport profiles in a manner such that the transport coefficients scale as would be expected by the
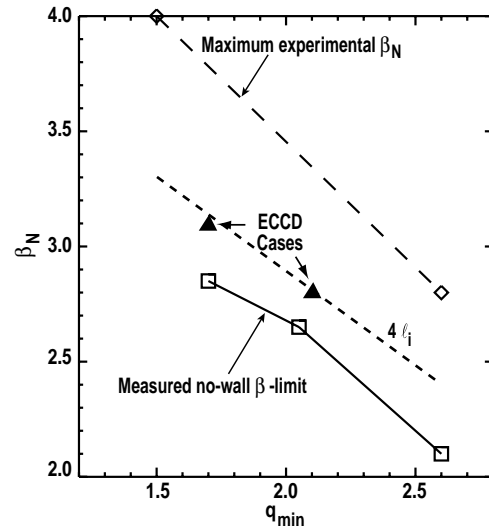
ITER H98-ELYy2 scaling expression ($\chi \sim \chi_{exp} P^{+0.69}$). The modeling indicates that with a modest increase in β from 3.3% in the ECCD case from Section II.B to 3.8% coupled with broadly distributed off-axis ECCD, fully non-inductive current drive with a steady-state current profile should be possible. Note that although this β value is 20% above the no-wall β limit, it is still 10% below the β achieved in Section III.A. The required NBI power to increase β to this level is predicted to be on the order of 12 MW though this is likely an overestimate since the modeling uses a fairly pessimistic transport scaling assumption. This NBI power level is well within the capabilities of the DIII–D NBI system.

In conclusion, recent experiments on DIII–D have demonstrated the feasibility of integrating the three main ingredients necessary for AT operation: stable, high β operation with $q_{min} \gg 1.5$, good energy confinement simultaneous with high β, and the ability to control the current profile via external means in high β plasmas. Operation well above the no-wall β limit is now routinely obtainable on DIII–D through the use of rotational stabilization of RWMs. In addition, off-axis ECCD has been shown to be an effective means of modifying and/or controlling the current density profile in high β plasmas. In the best case, non-inductive current fractions in excess of 90% have been demonstrated with up to 65% of the current produced by the self-generated bootstrap current. These results were made possible by an increasing understanding of the processes governing the underlying physics of these AT regimes. Advances in the understanding of stability (e.g. RWM stabilization, NTM avoidance), transport (e.g., E×B shear, negative shear stabilization), current drive (e.g., off-axis ECCD, bootstrap current), and particle control (e.g., wall inventory issues) as well as the interaction between these processes have been instrumental in the development of these AT regimes.

Acknowledgment

References

[1]   ITER Physics Basis, Nucl. Fusion **39**, 2137 (1999).
[2]   R.J. Bickerton et al., Nature (Phys. Sci.) **229**, 110 (1971).
[3]   C. Kessel, J. Manickam, G.W. Rewoldt, W.M. Tang, Phys. Rev. Lett. **72**, 1212 (1994).
[4]   A.D. Turnbull et al., Phys. Rev. Lett. **74**, 718 (1995).
[5]   T.S. Taylor et al, Plasma Phys. and Contr. Fusion **39**, B47 (1997).
[6]   R.E. Waltz et al., Phys. Plasmas **4**, 2482 (1997).
[7]   R.W. Harvey and M.G. McCoy in Proceedings of the IAEA Technical Committee Meeting, Montreal, 1992 (IAEA, Vienna, 1993)498.
[8]   C.C. Petty, this conference.
[9]   C.B. Forest et al., Phys. Rev. Lett. **73**, 2444 (1994).
[10]   M. Kotschenreuther, Bull. Am. Phys. Soc. **37**, 1432 (1992).
[11]   M.R. Wade et al., this conference.
[12]   M.R. Wade, et al., Phys. Plasmas **8**, 2208 (2001).
[13]   T.C. Luce et al., Nucl. Fusion **41**, 1585 (2001).
[14]   A.M. Garofalo, et al, Phys. Plasmas **9**, 1997 (2002).
[15]   D.P. Brennan et al, Phys. Plasmas **9**, 2998 (2002).
[16]   M. Murakami et al., submitted to Phys. Plasmas (2002).